Mixing ventilation strategy for an underground refuge during mine emergency

Shu Wang[1,2,a], Longzhe Jin[1,2,b*], Shengnan Ou[2,c], Zhiling Huang [1,d]

[1] School of Civil and Resource Engineering, University of Science and Technology Beijing, Beijing 100083, China

[2] Key Laboratory of Ministry of Education for Efficient Mining and Safety of Metal Mines, University of Science and Technology Beijing, Beijing 100083, China

[a] ustbwangshu@hotmail.com, [b] jinlongzhe-ustb@hotmail.com,

[c] osn@ustb.edu.cn, [d] bkdhzl@163.com

Abstract

Mechanical mixing ventilation (MV) systems have been commonly used in permanent refuge chambers (PRCs) to maintain sustainable environment for trapped miners during emergencies underground. For guiding the design of MV systems, in this study, 24 layouts with different combinations of the ventilation rate and number of diffusers were analyzed through simulations. The heat/carbon dioxide removal efficiencies, velocity non-uniform coefficient, local draft sensation, and thermal discomfort were calculated and discussed. Considering uncertain adverse circumstance during rescue, an optimal scheme with nine diffusers was proposed for a prototype. It is suggested the fresh air should be supplied at a minimum rate of 0.1 m^3/min per person, which can fulfill the basic living demands at the cost of thermal neutrality. A full-scale on-site experiment, in which critical environmental parameters and sick building syndrome (SBS) symptoms were recorded, was also performed to verify the rationality of the proposed ventilation scheme.

Keywords: Mine emergency; Permanent refuge chamber; Mechanically mixing ventilation; Air quality; Ventilation effectiveness; Thermal comfort

1. INTRODUCTION

Permanent refuge chambers (PRCs) are used to provide miners trapped underground during mine emergencies such as fire, explosions, or rock collapses with a well-sealed space that isolates them from a potentially toxic or high-temperature environment until it is safe to escape or until they are rescued (Margolis, Westerman and Kowalski-Trakofler, 2011; Mejías *et al.*, 2014; Z. Zhang *et al.*, 2018). For the safety of the miners, an adequate supply of oxygen and the control of harmful gas concentrations must be ensured within this confined space. Among all the strategies developed in recent years for sustainable environment maintenance, including physical and chemical methods (Jin *et al.*, 2015; Wang, Zhang and Jin, 2017), providing ventilation through pipelines from above the ground, though such pipelines may be destroyed during accidents in the underground mine, is decidedly the most cost effective.

Building ventilation has been systematically studied for over a hundred years worldwide, as it directly affects the indoor air quality and living comfort (Chenari, Dias Carrilho and Gameiro da Silva, 2016) by influencing the air flow pattern and airborne transmission/spread behavior in buildings (Li *et al.*, 2007; Nielsen *et al.*, 2010). Some researchers highlighted the association between sick building syndrome (SBS) symptoms and the ventilation rate (Sundell *et al.*, 2011; Tsai, Lin and Chan, 2012). To this end, different types of innovative air distribution systems have been developed in the past, such as mixing ventilation (MV), displacement ventilation (DV), personalized ventilation (PV), hybrid air distribution (HAD), and piston ventilation (PiV) systems. (Raftery *et al.*, 2015; Wang and Lin, 2015). As stated in Ref. (Cao *et al.*, 2014), each ventilation method has its merits and demerits, and it is suggested that the ventilation performance should be evaluated according to the specific objective of the system. Furthermore, several experimental and theoretical investigations have been performed to determine the most effective combination of critical parameters such as inlet and outlet positions, ventilation rate, and diffuser configurations (Khan *et al.*, 2006; Nastase *et al.*, 2011; Jurelionis *et al.*, 2015; Amai and Novoselac, 2016; Bragança *et al.*, 2016; Amai, Liu and Novoselac, 2017) for various applications.

However, for underground PRC, several restrictive conditions exist. The priority mission for a PRC is to provide a well confined safe space which is capable to protect miners from the outside hazards, like high temperature smoke, explosion blast, et al., in a mine emergency. Thus, the integrity of the concrete layer of the PRC should be maintained as much as possible. On the other hand, for the sealing purpose, the air outlet is designed as a U-bend buried pipe, which is restrained on the near-floor position because of its weight. Under such conditions, the use of mechanical MV systems, which supply fresh air through the ceiling diffusers

in the upper part of a PRC with high velocity to dilute excessive heat and pollutants within the living space (Shan *et al.*, 2016), is appropriate and reliable. In recent times, ceiling-diffuser-type MV systems have been commonly applied in PRCs, and relevant guidelines recommend a minimum fresh air flow rate of 0.3 m^3/min per capita. However, detailed instructions of ventilation systems were poorly mentioned.

To this end, in this study, a PRC at −375 m level in Kongzhuang coal mine in Jiangsu province was considered as a prototype. Both CFD calculation and on-site experiment were performed. The on-site test, with 100 adult males participated, was approved by the China Academy of Safety Science and Technology Review Board. The whole experimental duration, which lasted for 48 h, was divided into the three stages: (1) the passive stage, where the occupied zone was completely isolated from the external environment, with no fresh air replacement or air conditioning measures; (2) the mixing ventilation stage, where adequate fresh air was supplied through pipelines from above the ground, and (3) the air-regeneration stage, where the polluted air inside the occupied zone was purified by artificial means (air purifier, air conditioner, and compressed oxygen cylinder). Data sets of the second stage were used in this study.

With respect to the simulation study, two main factors important for the design of MV systems, namely, the ventilation rate and number of diffusers, were considered. A total of 24 layouts were analyzed using simulations and evaluated by comparing the corresponding ventilation efficiency including contaminant and heat removal, velocity non-uniform coefficient, predicted mean vote (*PMV*), and predicted percentage of dissatisfied (*PPD*). Several guiding instructions were summarized with the usability of PRCs during mine disasters taken as the precondition. Considering key factors such as the thermal comfort, ventilation efficiency, and uncertain adverse circumstance

during rescue, an optimal scheme was proposed. Further, a full-scale on-site experiment was performed to verify the proposed ventilation scheme.

2. NUMERICAL MODEL AND VALIDATION

2.1 Mathematical model.

A full-scale mathematical model was established, as shown in Figure 1. This chamber, with dimensions of 26.8 m (length, X axis) × 4.4 m (width, Z axis) × 3.7 m (height, Y axis), is capable of accommodating 100 miners. The side length of the square diffuser is 200 mm. Different simulation cases, with 5 to 13 diffusers mounted along the center line (X axis) at a height of 2800 mm (Y axis), were considered. Two air outlets, both circular with a radius of 150 mm, were positioned on each side. Other devices such as the purifier and drying cabinet were simplified as cube obstructions according to their actual sizes.

Miners inside the chamber were assumed to be in sedentary states, and were simplified into 400 mm × 200 mm × 900 mm (*L×W×H*) cubes according to the anthropometric data of 50th percentile Chinese

males in the sitting posture (China State Bureau of Technical Supervision, 1988). The gap between adjacent human bodies was ignored as miners were seated closely in the actual site. The flow pattern and heat transfer inside the gap do not significantly influence the domain of interest. The main hazards were considered to be the heat and carbon dioxide generated by miners living in the PRC. The total heat power per person was set as 75 W (Hajdukiewicz, Geron and Keane, 2013; Wang *et al.*, 2014). The carbon generation rate varied when miners under different activities during refuging (Ren *et al.*, 2017). Here, it was assumed that the human body exhales carbon dioxide steadily through the nose, and a averaged value of 0.6 L/min per person was used according to the data from the first stage of the on-site experiment. The area of nose opening for each miner was $4.2×10^{-4}$ m^2 (Ge *et al.*, 2013; Villafruela *et al.*, 2013; Yan *et al.*, 2016). The PRC envelope was constructed using reinforced concrete. The heat conductivity coefficient of the wall was 1.58 W/(m^2·K) (Hu *et al.*, 2008), and the surface temperature was set to 294 K, according to the site test result.
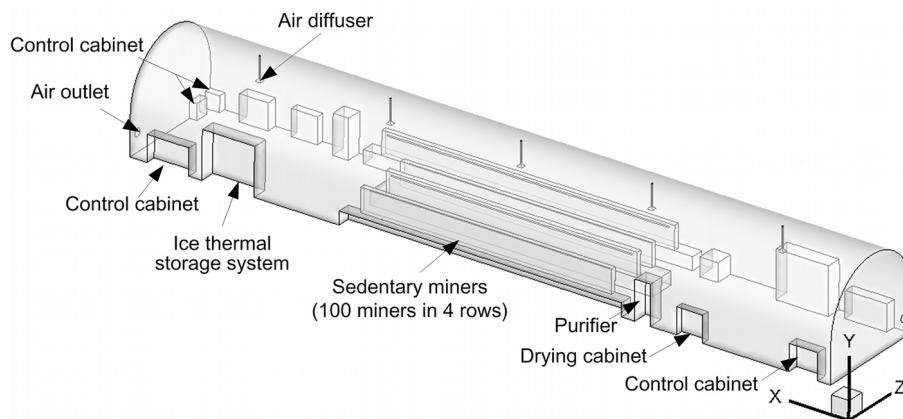

Fig. 1 Geometry of the CFD model extracted from the PRC at the site of the field experiment.

The turbulent flow and heat transfer in the domain were considered to be governed by the Reynolds-averaged Navier–Stokes (RANS) equation, generally expressed as follows (Inc., 2006):

$$\frac{\partial}{\partial t}(\rho\phi) = \frac{\partial}{\partial x_j}\left(\Gamma_\phi \frac{\partial\phi}{\partial x_j} - \rho u_j \phi\right) + S \tag{1}$$

where ϕ is the common dependent variable, ρ is the density, u is the velocity vector, Γ is the diffusion coefficient, and S_ϕ is the remaining term.

The RANS equation was solved numerically using the two-equation renormalized group RNG κ–ε turbulence model, owing to its advantages in terms of the accuracy, numerical stability, and short computing time, as shown in relevant work (Guo *et al.*, 2018); details concerning the RNG $k-\varepsilon$ model can be found in Ref. (Chen *et al.*, 2015). The SIMPLE algorithm was applied to solve the nonlinearity of the momentum equation, the velocity–pressure coupling, and the coupling between the flow momentum and energy equations (Horikiri, Yao and Yao, 2014). Air in the domain was considered as incompressible gas. A body force weighted pressure interpolation scheme was employed (Horikiri, Yao and Yao, 2012). The PRESTO! discretization was used for pressure solving (Zhou *et al.*, 2017). The second-order upwind discretization scheme was chosen to solve other variables (Zheng and Liu, 2015). Enhanced wall treatment was applied to the near-wall cells (Ahmed and Gao, 2017).The circular air outlet represented the outflow boundary. The diffusion of carbon dioxide was determined by using a species transport model with no reaction. Steady calculation was performed, and the convergence criteria was selected as 10^{-6} for the residual energy and 10^{-3} for all other parameters.

2.2 Computational cases and data processing.

A total of 24 cases with different combinations of ventilation rate (Q) and number of diffusers (N) were simulated, as tabulated in Table 1. A ventilated cell was defined as the region covered by a single diffuser, and the central line between two adjacent diffusers was the edge of the ventilated cells (Foat, Nally and Parker, 2017). The aspect ratio (length/width) of the cell was then introduced to represent different ventilation configurations. For all the configurations, considering the environment condition on site, the initial temperature inside the
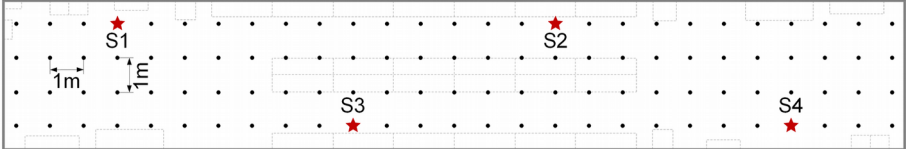
domain was 298 K, the temperature of fresh air supplied through the diffusers was 298 K.

In all cases, a set of 108 monitoring points located at the inhalation height (nose level, $Y = 1.2$ m) were used for assessment, as shown in Figure 2. Four points (S1–S4) among these were considered to compare the results between computational and site experiment studies to enable model validation.

Table 1

Description of simulation cases

Case No.	Aspect ratio of ventilated cell	300	600	900	1200	1500	1800
5	1.14	A-1	A-2	A-3	A-4	A-5	A-6
7	0.91	B-1	B-2	B-3	B-4	B-5	B-6
9	0.68	C-1	C-2	C-3	C-4	C-5	C-6
13	0.45	D-1	D-2	D-3	D-4	D-5	D-6

(Number of diffusers)

Fig. 2 Monitoring points (dot symbol) for simulation cases. The red stars indicate the four monitoring locations considered in site experiment (all points lie in the inhalation zone pertaining to a sitting posture, Y = 1.2 m).

To evaluate the global effectiveness of different ventilation layouts, two ventilation performance indices, namely, the contaminant removal effectiveness (ε_c) (Berlanga *et al.*, 2018) and temperature effectiveness (ε_T) (Amai, Liu and Novoselac, 2017; S. Zhang *et al.*, 2018) were considered. The values of ε_c and ε_T were calculated using the following expressions:

$$\varepsilon_c = \frac{c_e - c_s}{\overline{c} - c_s} \times 100 \, [\%] \tag{2}$$

$$\varepsilon_T = \frac{T_e - T_s}{\overline{T} - T_s} \times 100 \, [\%] \tag{3}$$

where, $\overline{c}$, c_e, and c_s represent the mean concentrations in the chamber, exhaust, and supply, respectively (in vol %). $\overline{T}$, T_e, and T_s represent the

mean temperatures in the chamber, exhaust, and supply, respectively (K).

The predicted mean vote (*PMV*) and predicted percentage of dissatisfied (*PPD*) parameters were introduced to indicate the indoor thermal comfort. The PMV represents the mean value of the voters of a population in the same environment on a seven-point thermal sensation scale from cold (-3) to hot (+3), considering a particular combination of air temperature, mean radiant temperature, relative humidity, air speed, metabolic rate, and clothing insulation. The PPD value is an index representing the percentage of thermally dissatisfied persons. The values of PMV and PPD were calculated using the following expressions (Horikiri, Yao and Yao, 2015):

$$PPD = 100 - 95 \times e^{-(0.03353 \times PMV^4 + 0.2179 \times PMV^2)} \tag{4}$$

$$
\begin{aligned}
PMV = {} & (0.03e^{-0.036M} + 0.028)\{(M - W) - 3.05 \times 10^{-3} \times [5733 - 6.99(M - W) - p_a] \\
& - 0.42 \times [(M - W) - 58.15] - 17 \times 10^{-5} M (5867 - p_a) - 0.0014M(34 - t_a) \\
& - 3.96 \times 10^{-8} f_{cl} \times [(t_{cl} + 273)^4 - (\overline{t_r} + 273)^4] - f_{cl} h_c (t_{cl} - t_a)\}
\end{aligned}
\tag{5}
$$

$$t_{cl} = 35.7 - 0.028(M - W) - c_{cl}\{3.96\times10^8 f_{cl} \times [(t_{cl} + 273)^4 - (\bar{t}_r + 273)^4] + f_{cl}h_c(t_{cl} - t_a)\} \tag{6}$$

$$h_c = \begin{cases} 2.38(t_{cl} - t_a)^{0.25} & 2.38(t_{cl} - t_a)^{0.25} > 12.2\sqrt{v_{ar}} \\ 12.2\sqrt{v_{ar}} & \text{for } 2.38(t_{cl} - t_a)^{0.25} < 12.2\sqrt{v_{ar}} \end{cases} \tag{7}$$

$$f_{cl} = \begin{cases} 1.00 + 1.290 I_{cl} & I_{cl} \le 0.078(\text{m}^2 \cdot{}^\circ\text{C/W}) \\ 1.05 + 0.645 I_{cl} & \text{for } I_{cl} > 0.078(\text{m}^2 \cdot{}^\circ\text{C/W}) \end{cases} \tag{8}$$

where M is the metabolic rate, 69.78 W/m^2 for sedentary level (Kabanshi, Wigö and Sandberg, 2016); W represents the external work, 0 W/m^2; p_a is the partial water vapor pressure, Pa; t_a is the air temperature, °C; f_{cl} is the ratio of a body's clothed surface area over the naked surface area; I_{cl} is clothing insulation, m^2·°C/W—here, the value was set to 1.1 clo according to ASHRAE (ASHRAE, 2013); t_{cl} is the surface temperature of clothing, °C; $\bar{t}_r$ is the mean radiant temperature, °C; h_c is the convective heat transfer coefficient, W/m^2·°C; and v_{ar} is the relative air velocity with reference to a human body, m/s.

In addition, using the local air velocity values at 108 monitoring points, the velocity non-uniform coefficient (k_u, dimensionless) was obtained to evaluate the distribution of airflow at the height of the inhalation level, using the following expression (Li *et al.*, 2011):

$$k_u = \frac{s_u}{\bar{u}} = \frac{\sqrt{\sum (u_i - \bar{u})^2 / n}}{\bar{u}} \tag{9}$$

where σ_u is the velocity standard deviation; $\bar{u}$ is the average velocity; and n is the number of monitoring points.

2.3 Model validation.

C-2 model was used for model validation. A grid independent study was conducted using three successive grid resolutions of 29.4×10^4, 39.9×10^4, and 50.2×10^4 grid points. The volume averaged air temperatures were 302.43, 301.82, and 301.79 K. Thus, the 39.9×10^4-grid system was selected in this study. Then, a comparison between the

experimental and predicted values of the local temperature and concentration of carbon dioxide at points S1–S4 is presented in Figure 3. The computed temperatures can be noted to agree with the measured value within 1.35 K, and the concentrations are within 0.07 %, which demonstrates the reliability of the numerical model.
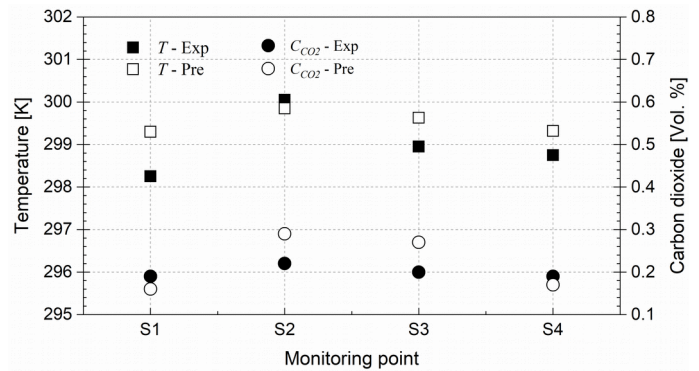
Fig. 3 Comparison of temperatures and concentrations of carbon dioxide at four monitoring locations in the site experiment and simulation.

3. RESULTS AND DISCUSSION

3.1 Simulation results of 24 layouts.

Figure 4 shows the calculated averaged results of the 24 layouts. In all cases, the averaged carbon dioxide level ($\bar{c}$) and temperature ($\bar{T}$) inside the computed zone were less than 1% and 308.15 K, respectively, which are the limits specified in the relevant standards of PRCs. It can be observed that $\bar{c}$ and $\bar{T}$ were inversely proportional to Q and N, with minimum values of 0.20% and 298.97 K, respectively, when $Q = 1800$ m^3/h and $N = 13$ (Case D-6). The carbon dioxide level and temperature distribution of vertical slices in the figures

presented in the Appendix indicate that higher temperature and contaminant gradients were present in the upper region in Case A-1, and stratification was eliminated with increase in Q and N. It can be intuitively concluded that the lower inlet clean air

momentum could not neutralize the heat and mass combined buoyancy forces generated by miners; however, higher flow rates could mix and dilute the heat and contaminant in the occupied zone.
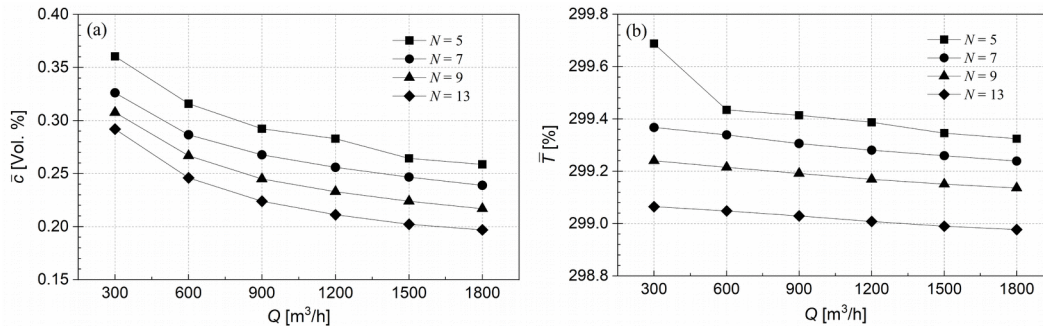

Fig. 4 Results for the 24 layouts: (a) averaged carbon dioxide level ($\overline{c}$); (b) averaged temperature ($\overline{T}$).
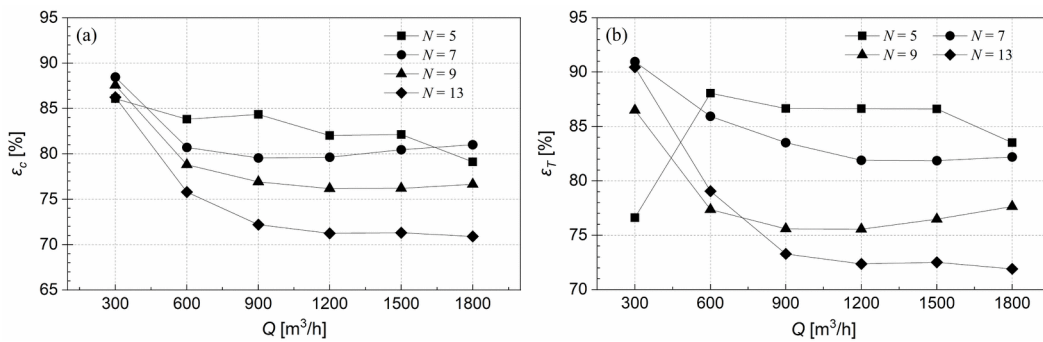

Fig. 5 Ventilation effectiveness of 24 layouts: (a) contaminant removal effectiveness represented by carbon dioxide ($\mathcal{E}_c$); (b) temperature effectiveness ($\mathcal{E}_T$).
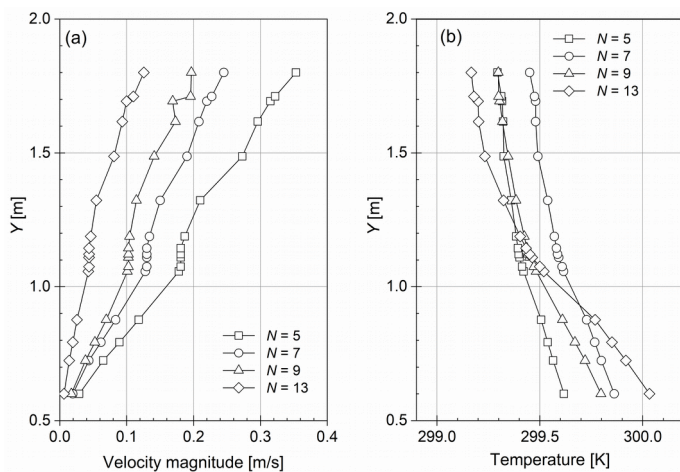
Fig. 6 Vertical distributions with different number of diffusers when ventilation rate is 900 m^3/h: (a) velocity magnitude; (b) temperature.

3.2 Ventilation effectiveness.

The ventilation efficiencies for the contaminant and heat removal ($\mathcal{E}_c$ and $\mathcal{E}_T$) were calculated using Eqs. (2) and (3). Figure 5 illustrates the results of different configurations. It can be noted that better utilization of fresh air was achieved when Q was 300 m^3/h, and N did not exert considerable influence on the performance. When $Q > 900$ m^3/h, the ventilation efficiencies of layouts with the same N remained nearly constant, indicating that N was the dominant factor, and better utilization of fresh

air could be achieved by decreasing the number of diffusers.

Figure 6 shows the vertical profiles of the velocity magnitude, temperature, and carbon dioxide levels in the center of the PRC when $Q = 900$ m^3/h. The curves suggest that a higher vertical velocity gradient occurs with decrease in N. The maximum difference between the velocities at heights of 0.6 m and 1.8 m was 0.32 m/s in Case A-3, indicating that a low N may generate drafting sensation in the local areas under the diffusers, owing to the strong air motions induced in that region.

3.3 Velocity non-uniform coefficient pertaining to inhalation height.

Figure 7 shows the velocity non-uniform coefficients of different ventilation configurations at the inhalation height of the prototype, Y = 1.2 m. It can be found that k_u was mainly affected by N, and it changed only slightly with Q. Layout groups with $N = 13$ produced the minimum value of k_u, with an average of approximately 0.42. The velocity at the inhalation height was in the range of 0.009–0.172 m/s, directly proportional to Q. When $N = 5$, the averaged value of k_u for Cases A-1 to A-6 was 0.66, and the velocity was in the range of 0.011–0.406 m/s.
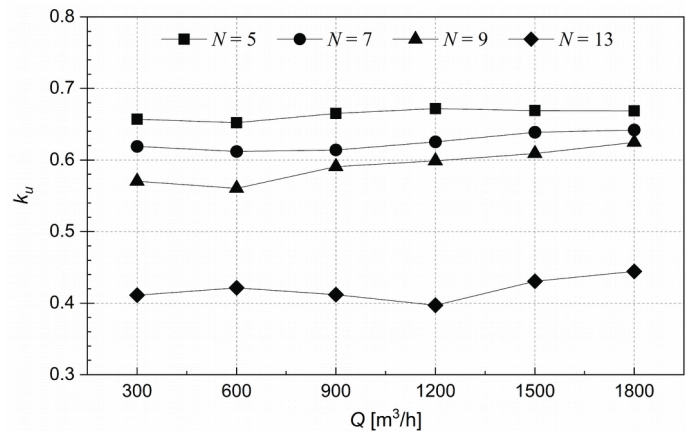

Fig. 7 Velocity non-uniform coefficient (k_u) at the inhalation height ($Y = 1.2$ m).

3.4 Thermal comfort PMV and PPD pertaining to inhalation height.

The PMV and PPD values of the 24 studied layouts were calculated at the inhalation height by using Eqs. (4)–(8), as shown in Figure 8. The cases with a higher ventilation rate demonstrated improved thermal comfort. The value of $Q = 1800$ m^3/h corresponded to an overall *PMV* of 0.45 and *PPD* of 9.25% at the inhalation height for sitting miners, which is close to the thermal neutrality condition. At $Q = 300$ m^3/h, the overall *PMV* and *PPD* at the inhalation height increased to 1.16 and 36.92%, respectively, representing a thermal sensation of "more than slightly warm".
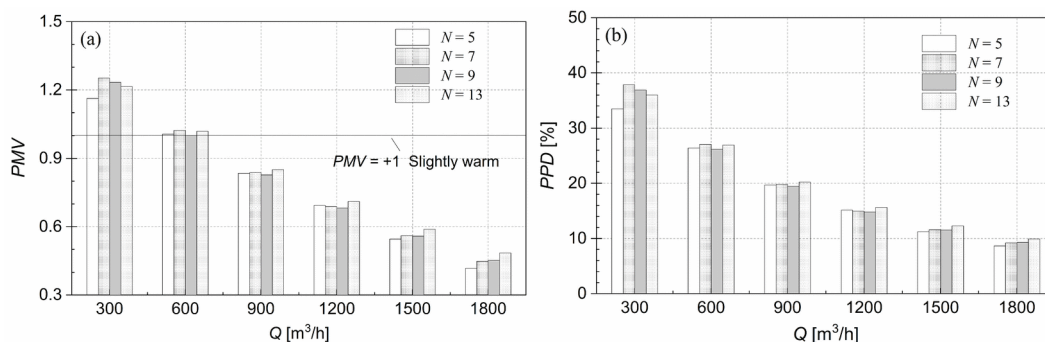

Fig. 8 Thermal comfort results of 24 layouts: (a) predicted mean vote (PMV); (b) predicted percentage of dissatisfied (PPD).

In an unpredictable disaster scenario, it is difficult to guarantee an air supply rate of 1800 m^3/h for a long period of time for a typical PRC with a normally rated accommodation of 100 persons.

3644

ASHRAE Standard 55-2010 recommends that the requirement of at least 80% of the occupants should be satisfied for indoor thermal conditions. Further, in specific emergency rescue scenarios during underground disasters, it is recommended that the *PPD* can extended to 30%, taking both energy conservation and living demand into consideration. Thus, in the studied prototype, a minimum Q value of 600 m³/h is recommended, as it can satisfy both the living and thermal comfort requirements during a disaster.

Change in N had a slight effect on the *PMV* or *PPD* when Q remained constant. As stated previously, increasing the number of diffusers may lead to improvements in terms of the draft sensation; but increasing the number of diffusers might lead to an infeasible design of stepped air-supply pipelines and excessive noise, from a practical point of view. Take an overall consideration, a design scheme with nine diffusers was thus proposed for the studied prototype.

4. ON-SITE EXPERIMENTAL INVESTIGATION

An on-site experiment was conducted in a PRC at −375 m level in Kongzhuang coal mine in Jiangsu province, with 100 adult males aged 37.2 ± 8.45 years. The study was approved by the China Academy of Safety Science and Technology Review Board. All the participants were aware of the environmental parameters throughout the tests. Only ship biscuit (5000 kJ per day per man) and drinking water (1.5 L per day per man) were supplied during the tests to simulate a rescue scenario.

Fig. 9 On-site ventilation experiment and questionnaires (red arrows represented the positions of monitoring points).
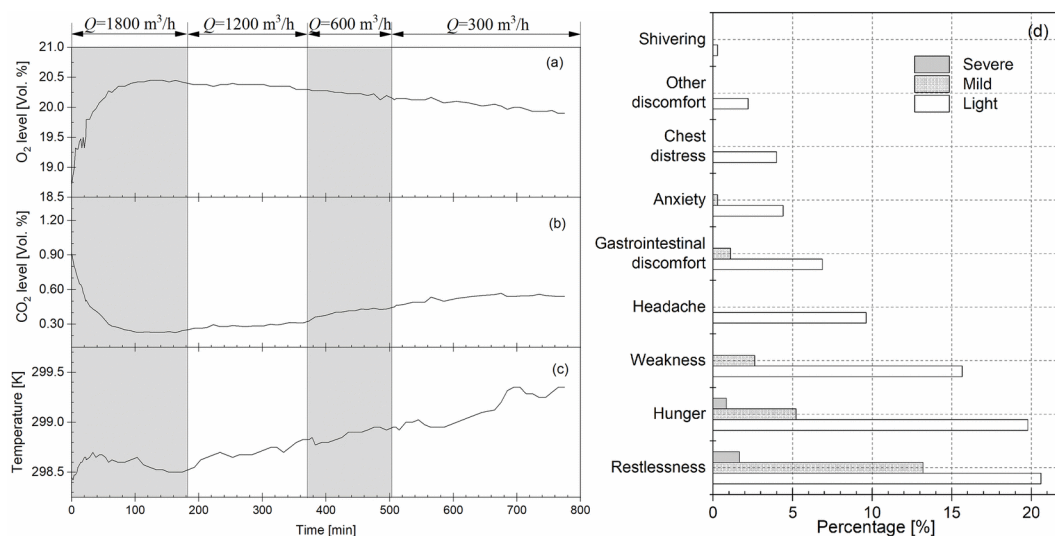

Fig. 10 Evolution of critical environmental parameters with time during on-site experiment: (a) oxygen level; (b) carbon dioxide level; (c) temperature; (d) sick building syndromes of participants.

The duration of the ventilation evaluation, which is the second stage as mentioned before, was approximately 775 min. It was noted that the initial oxygen and carbon dioxide levels of the this stage were 18.7 vol.% and 0.91 vol.%, respectively. Four different ventilation rates (1800 m^3/h, 1200 m^3/h, 600 m^3/h, 300 m^3/h respectively) were employed. Four points (S1–S4) at the inhalation height (nose level, $Y = 1.2$ m) were monitored through the supervisory control and data acquisition (SCADA) system in real time, see in Figure 9. The environmental parameters pertaining to oxygen, carbon dioxide, and temperature evolution are illustrated in Figure 10. All the parameters were within the range of the limits specified in the relevant standards of PRCs ($O_2 > 18.5$ vol %; $CO_2 < 1.0$ vol %; temperature < 303 K). SBS statistics from the feedback of the participants are also presented. The symptoms considering the physical condition were mainly light level sleepiness, hunger, weakness, and gastrointestinal discomfort, mainly because of the long duration of the on-site experiment. In general, recommended air flow rate of 0.3 m^3/min per capita can restore the oxygen deficient environment to normal level within 1 h; while an air flow rate of 0.1 m^3/min per person could guarantee the basic living demands at the cost of thermal neutrality. This rate is also energy efficient.

5. CONCLUSION

In this study, the ventilation performance of different MV layouts of a PRC utilized in specific underground disasters was investigated. By performing an on-site experiment and simulation analysis, the following conclusions could be derived:

(1) The averaged carbon dioxide level and temperature inside the confined rescue space were inversely proportional to the inlet air flow rate and number of diffusers. Under the same ventilation rate, better utilization of fresh air could be achieved when the number of diffusers decreased; but a local draft sensation or thermal discomfort for the miners sitting under the diffuser may occur.

(2) Higher ventilation rate demonstrated improvement of the thermal comfort; while the number of diffusers did not exhibit a significant effect when the inlet air flow rate remained constant in the studied prototype.

(3) Considering both the energy conservation and living demands in specific emergency rescue scenarios during underground mine disasters, ventilation scheme with nine diffusers was proposed for the studied PRC. Fresh air was recommended be supplied at a minimum rate of 0.1 m^3/min per person, as it can fulfill the basic living demands at the cost of thermal neutrality, especially in the uncertain adverse circumstance during rescue.

ACKNOWLEDGEMENTS

REFERENCES

[1] Ahmed, A. Q. and Gao, S. (2017) 'Numerical investigation of height impact of local exhaust combined with an office work station on energy saving and indoor environment', *Building and Environment*. Pergamon, 122, pp. 194–205. doi: 10.1016/J.BUILDENV.2017.06.011.

[2] Amai, H., Liu, S. and Novoselac, A. (2017) 'Experimental study on air change effectiveness: Improving air distribution with all-air heating systems', *Building and Environment*. Pergamon,

125, pp. 515–527. doi: 10.1016/J.BUILDENV. 2017.09.017.

[3] Amai, H. and Novoselac, A. (2016) 'Experimental study on air change effectiveness in mixing ventilation', *Building and Environment*. Pergamon, 109, pp. 101–111. doi: 10.1016/ J. BUILDENV.2016.09.015.

[4] ASHRAE (2013) *2013 ASHRAE Handbook: Fundamentals, Design*. doi: 10.1163/ej. 9789004155947.i-937.23.

[5] Berlanga, F. A. *et al.* (2018) 'Experimental assessment of different mixing air ventilation systems on ventilation performance and exposure to exhaled contaminants in hospital rooms', *Energy and Buildings*. Elsevier, 177, pp. 207–219. doi: 10.1016/J.ENBUILD. 2018.07.053.

[6] Bragança, P. *et al.* (2016) 'Airflow characteristics and thermal comfort generated by a multi-cone ceiling diffuser with and without inserted lobes', *Building and Environment*. Pergamon, 108, pp. 143–158. doi: 10.1016/J. BUILDENV. 2016.08.029.

[7] Cao, G. *et al.* (2014) 'A review of the performance of different ventilation and airflow distribution systems in buildings', *Building and Environment*. Pergamon, 73, pp. 171–186. doi: 10.1016/J.BUILDENV.2013.12.009.

[8] Chen, H. *et al.* (2015) 'Numerical investigation of ventilation performance of different air supply devices in an office environment', *Building and Environment*. Pergamon, 90, pp. 37–50. doi: 10.1016/J.BUILDENV.2015.03.021.

[9] Chenari, B., Dias Carrilho, J. and Gameiro da Silva, M. (2016) 'Towards sustainable, energy-efficient and healthy ventilation strategies in buildings: A review', *Renewable and Sustainable Energy Reviews*. Pergamon, 59, pp. 1426–1447. doi: 10.1016/J.RSER.2016.01.074.

[10] China State Bureau of Technical Supervision (1988) *Human dimensions of Chinese adults, GB 10000 88*. Beijing, China.

[11] Foat, T. G., Nally, J. and Parker, S. T. (2017) 'Investigating a selection of mixing times for transient pollutants in mechanically ventilated, isothermal rooms using automated computational fluid dynamics analysis', *Building and Environment*. Pergamon, 118, pp. 313–322. doi: 10.1016/J.BUILDENV. 2017. 01.011.

[12] Ge, Q. *et al.* (2013) 'Numerical study of the effects of human body heat on particle transport and inhalation in indoor environment', *Building and Environment*. Pergamon, 59, pp. 1–9. doi: 10.1016/J.BUILDENV.2012.08.002.

[13] Guo, P. *et al.* (2018) 'Reduced-scale experimental model and numerical investigations to buoyance-driven natural ventilation in a large space building', *Building and Environment*. Pergamon, 145, pp. 24–32. doi: 10.1016/J. BUILDENV.2018.09.019.

[14] Hajdukiewicz, M., Geron, M. and Keane, M. M. (2013) 'Formal calibration methodology for CFD models of naturally ventilated indoor environments', *Building and Environment*, 59, pp. 290–302. doi: 10.1016/j.buildenv. 2012.08.027.

[15] Horikiri, K., Yao, Y. and Yao, J. (2012) 'Numerical study of unsteady airflow phenomena in a ventilated room', *Proceedings of CHT-12. ICHMT International Symposium on Advances in Computational Heat Transfer. July 1-6, 2012, Bath, England*. Begel House Inc. Available at: http://www.dl.begellhouse.com/references/1bb3 31655c289a0a,636c91ea5ddcad95,153299381f1 2ac04.html?year=2015 (Accessed: 3 May 2019).

[16] Horikiri, K., Yao, Y. and Yao, J. (2014) 'Modelling conjugate flow and heat transfer in a ventilated room for indoor thermal comfort assessment', *Building and Environment*. Pergamon, 77, pp. 135–147. doi: 10.1016/J.BUILDENV.2014.03.027.

[17] Horikiri, K., Yao, Y. and Yao, J. (2015) 'Numerical optimisation of thermal comfort

improvement for indoor environment with occupants and furniture', *Energy and Buildings*. Elsevier, 88, pp. 303–315. doi: 10.1016/J.ENBUILD.2014.12.015.

[18] Hu, L. H. *et al.* (2008) 'Confinement of fire-induced smoke and carbon monoxide transportation by air curtain in channels', *Journal of Hazardous Materials*. Elsevier, 156(1–3), pp. 327–334. doi: 10.1016/J.JHAZMAT.2007.12.041.

[19] Inc., F. (2006) *Fluent 6.3 - User's guide*, *Fluent Inc.* doi: 10.1016/0167-4048(92)90125-B.

[20] Jin, L. Z. *et al.* (2015) 'Development of a low oxygen generation rate chemical oxygen generator for emergency refuge spaces in underground mines', *Combustion Science and Technology*, 187(8), pp. 1229–1239. doi: 10.1080/00102202.2015.1031223.

[21] Jurelionis, A. *et al.* (2015) 'The impact of the air distribution method in ventilated rooms on the aerosol particle dispersion and removal: The experimental approach', *Energy and Buildings*. Elsevier, 86, pp. 305–313. doi: 10.1016/ J.ENBUILD.2014.10.014.

[22] Kabanshi, A., Wigö, H. and Sandberg, M. (2016) 'Experimental evaluation of an intermittent air supply system – Part 1: Thermal comfort and ventilation efficiency measurements', *Building and Environment*. Pergamon, 95, pp. 240–250. doi: 10.1016/J.BUILDENV.2015.09.025.

[23] Khan, J. A. *et al.* (2006) 'Effects of inlet and exhaust locations and emitted gas density on indoor air contaminant concentrations', *Building and Environment*, 41(7), pp. 851–863. doi: 10.1016/j.buildenv.2005.04.002.

[24] Li, A. *et al.* (2011) 'Reduced-scale model study of ventilation for large space of generatrix floor in HOHHOT underground hydropower station', *Energy and Buildings*. Elsevier, 43(4), pp. 1003–1010. doi: 10.1016/J.ENBUILD. 2010.12.026.

[25] Li, Y. *et al.* (2007) 'Role of ventilation in airborne transmission of infectious agents in the built environment - a multidisciplinary systematic review.', *Indoor air*, 17(1), pp. 2–18. doi: 10.1111/ j.1600-0668.2006.00445.x.

[26] Margolis, K. A., Westerman, C. Y. K. and Kowalski-Trakofler, K. M. (2011) 'Underground mine refuge chamber expectations training: program development and evaluation', *Safety Science*, 49, pp. 522–530. doi: 10.1016/j.ssci.2010.12.008.

[27] Mejías, C. *et al.* (2014) 'Clinical response of 20 people in a mining refuge: Study and analysis of functional parameters', *Safety Science*. Elsevier, 63, pp. 204–210. doi: 10.1016/J.SSCI. 2013.11.011.

[28] Nastase, I. *et al.* (2011) 'Lobed grilles for high mixing ventilation – An experimental analysis in a full scale model room', *Building and Environment*. Pergamon, 46(3), pp. 547–555. doi: 10.1016/J.BUILDENV.2010.08.008.

[29] Nielsen, P. V. *et al.* (2010) 'Risk of cross-infection in a hospital ward with downward ventilation', *Building and Environment*. Pergamon, 45(9), pp. 2008–2014. doi: 10.1016/ J.BUILDENV.2010.02.017.

[30] Raftery, P. *et al.* (2015) 'Laboratory testing of a displacement ventilation diffuser for underfloor air distribution systems', *Energy and Buildings*. Elsevier, 108, pp. 82–91. doi: 10.1016/ J.ENBUILD. 2015.09.005.

[31] Ren, Z. *et al.* (2017) 'Respiration-related parameters and comfort levels of miners during refuge in underground mines', *Boletin Tecnico/Technical Bulletin*. Universidad Central de Venezuela, 55(9), pp. 636–643. Available at: https://www.engineeringvillage.com/share/docu ment.url? mid=cpx_M287557a215f6da5af0dM6bf010178 163176&database=cpx.

[32] Shan, X. *et al.* (2016) 'Comparing mixing and displacement ventilation in tutorial rooms:

Students' thermal comfort, sick building syndromes, and short-term performance', *Building and Environment*. Pergamon, 102, pp. 128–137. doi: 10.1016/J.BUILDENV. 2016.03.025.

[33] Sundell, J. *et al.* (2011) 'Ventilation rates and health: multidisciplinary review of the scientific literature', *Indoor Air*. John Wiley & Sons, Ltd (10.1111), 21(3), pp. 191–204. doi: 10.1111/j.1600-0668.2010.00703.x.

[34] Tsai, D.-H., Lin, J.-S. and Chan, C.-C. (2012) 'Office Workers' Sick Building Syndrome and Indoor Carbon Dioxide Concentrations', *Journal of Occupational and Environmental Hygiene*. Taylor & Francis Group , 9(5), pp. 345–351. doi: 10.1080/15459624.2012.675291.

[35] Villafruela, J. M. *et al.* (2013) 'CFD analysis of the human exhalation flow using different boundary conditions and ventilation strategies', *Building and Environment*. Pergamon, 62, pp. 191–200. doi: 10.1016/J.BUILDENV. 2013.01.022.

[36] Wang, S., Zhang, T. and Jin, L. (2017) 'Revitalization of air using a potassium superoxide plate in hypoxic space: Performance and kinetic model under natural convection conditions', *Indoor and Built Environment*, p. 1420326X17705944. doi: 10.1177/ 1420326X17705944.

[37] Wang, X. and Lin, Z. (2015) 'An experimental investigation into the pull-down performances with different air distributions', *Applied Thermal Engineering*. Pergamon, 91, pp. 151–162. doi: 10.1016/J. APPLTHERMALENG. 2015.08.012.

[38] Wang, Y. *et al.* (2014) 'Classroom energy efficiency and air environment with displacement natural ventilation in a passive public school building', *Energy and Buildings*. Elsevier, 70, pp. 258–270. doi: 10.1016/J. ENBUILD. 2013.11.071.

[39] Yan, Y. *et al.* (2016) 'Evaluation of manikin simplification methods for CFD simulations in occupied indoor environments', *Energy and Buildings*. Elsevier, 127, pp. 611–626. doi: 10.1016/J.ENBUILD.2016.06.030.

[40] Zhang, S. *et al.* (2018) 'Dynamic control of room air temperature for stratum ventilation based on heat removal efficiency: Method and experimental validations', *Building and Environment*. Pergamon, 140, pp. 107–118. doi: 10.1016/J.BUILDENV.2018.05.029.

[41] Zhang, Z. *et al.* (2018) 'Thermal performance analysis of an underground closed chamber with human body heat sources under natural convection', *Applied Thermal Engineering*, 145, pp. 453–463. doi: https://doi.org/10.1016/j. applthermaleng. 2018.09.068.

[42] Zheng, C. and Liu, J. (2015) 'Study on indoor air movement under the crowding conditions by numerical simulations and PIV small-scale experiments', *Procedia Engineering*. Elsevier, 121, pp. 1650–1656. doi: 10.1016/J.PROENG. 2015.09.109.

[43] Zhou, Y. *et al.* (2017) 'The effects of ventilation and floor heating systems on the dispersion and deposition of fine particles in an enclosed environment', *Building and Environment*. Pergamon, 125, pp. 192–205. doi: 10.1016/J. BUILDENV. 2017.08.049.